

# PCCP

Physical Chemistry Chemical Physics

Accepted Manuscript

This article can be cited before page numbers have been issued, to do this please use: F. Martinez, N. S. Adler, C. N. Cavasotto and G. A. Aucar, *Phys. Chem. Chem. Phys.*, 2022, DOI: 10.1039/D2CP00398H.



This is an Accepted Manuscript, which has been through the Royal Society of Chemistry peer review process and has been accepted for publication.

Accepted Manuscripts are published online shortly after acceptance, before technical editing, formatting and proof reading. Using this free service, authors can make their results available to the community, in citable form, before we publish the edited article. We will replace this Accepted Manuscript with the edited and formatted Advance Article as soon as it is available.

You can find more information about Accepted Manuscripts in the [Information for Authors](#).

Please note that technical editing may introduce minor changes to the text and/or graphics, which may alter content. The journal's standard [Terms & Conditions](#) and the [Ethical guidelines](#) still apply. In no event shall the Royal Society of Chemistry be held responsible for any errors or omissions in this Accepted Manuscript or any consequences arising from the use of any information it contains.

Cite this: DOI: 00.0000/xxxxxxxxxx

## Solvent effects on the NMR shieldings of stacked DNA base pairs<sup>†</sup>

Fernando A. Martínez,<sup>a,b</sup> Natalia S. Adler,<sup>c,d</sup> Claudio N. Cavasotto<sup>c,e,f</sup> and Gustavo A. Aucar<sup>\*a,g</sup>

Received Date

Accepted Date

DOI: 00.0000/xxxxxxxxxx

Stacking effects are among the most important ones in DNA. We have recently studied its influence in fragments of DNA through the analysis of NMR magnetic shieldings, firstly in vacuo. As a continuation of this line of research we show here the influence of solvent effects on those shieldings through the application of both, explicit and implicit models. We found that the explicit solvent model is the most appropriate to consider due to results match in general better with experiments and also one get a clear knowledge of the electronic origin of the value of the shieldings. Our study is grounded on a recently developed theoretical model of our own, by which we are able to learn about magnetic effects of given fragments of DNA molecules on selected base pairs. We use the shieldings of the atoms of a central base pair (guanine-cytosine) of a selected fragment of DNA molecules as descriptors of physical effects, like  $\pi$ -stacking and solvent. They can be taken separately and altogether. The former is introduced through the addition of some pairs above and below of the central one, and now, the latter is considered including a network of water molecules that consist of two solvation layers which were fixed in the calculations performed in all fragments. We show that solvent effects enhance the stacking effects on magnetic shieldings of atoms that belongs to the external N–H bonds. The net effect is of deshielding on both atoms. There is also a deshielding effect on Carbon atoms that belongs to C=O bonds for which the Oxygen atom has an explicit HB with a solvent water molecule. Solvent effects are found to be not higher than few percent of the total value of shieldings (between 1% to 5%) for most atoms, but there are few for which such effect can be higher. There is one nitrogen atom, the acceptor of the HB between guanine and cytosine, that is highly more shielded (around 15 ppm or 10%) when the explicit solvent is considered. In a similar manner the most external nitrogen atom of cytosine and the Hydrogen atom that is bonded to it, are highly deshielded (around 10 ppm for nitrogen and around 3 ppm for Hydrogen).

## 1 Introduction

Non-covalent inter- and intra-molecular interactions involving aromatic rings are present in a large number of chemical and biological processes: molecular recognition, self-assembly, catalysis

and transport.<sup>1,2</sup> They are fundamental in the stacking of base pairs in DNA<sup>3</sup>, and contribute to the structure of proteins and to protein-ligand interaction.<sup>4</sup>

Aromatic interactions are considered to consist of van der Waals and electrostatic forces.<sup>5,6</sup> The relative contribution and magnitude of each of these interactions is still under study, but it is known that they are not as different from simple interactions as Hydrogen bonds (HBs) are. Although the electrostatic principles that govern the magnitudes of HB also apply to aromatic interactions, there are some other points of contact where electrostatic interactions must be considered, so that it is difficult to rationalize the behavior of aromatic interactions with simple rules as occurs in the case of HB.<sup>6</sup> However, beyond the fact that many supramolecular interactions are generally classified as non-covalent, recent studies have shown that certain interactions are stabilized by a very important covalent component,<sup>7</sup> and are governed by orbital interactions<sup>8</sup> that imply a significant electron

<sup>a</sup> Institute of Modelling and Innovation on Technology (IMIT), CONICET-UNNE<sup>b</sup> Chemistry Department, Natural and Exact Science Faculty, Northeastern University of Argentina, Avda Libertad 5460, W3404AAS Corrientes, Argentina<sup>c</sup> Computational Drug Design and Biomedical Informatics Laboratory, Instituto de Investigaciones en Medicina Translacional (IIMT), CONICET-Universidad Austral, Pilar, Buenos Aires, Argentina<sup>d</sup> Centro de Investigaciones en BioNanociencias (CIBION), CONICET, Buenos Aires, Argentina<sup>e</sup> Facultad de Ciencias Biomédicas and Facultad de Ingeniería, Universidad Austral, Pilar, Buenos Aires, Argentina<sup>f</sup> Austral Institute for Applied Artificial Intelligence, Universidad Austral, Pilar, Buenos Aires, Argentina<sup>g</sup> Physics Department, Natural and Exact Science Faculty, Northeastern University of Argentina, Avda Libertad 5460, W3404AAS Corrientes, Argentina; email:gaucar@conicet.gov.ar

sharing and charge transfer.<sup>9,10</sup> It is worth to emphasize that the application of quantum mechanics (QM) play an important role for describing electronic effects when biomolecular interactions are involved.<sup>11–13</sup>

The calculation of NMR parameters has contributed significantly to the understanding of molecular interactions involving bases of DNA and RNA.<sup>14</sup> As discussed in a previous publication<sup>15</sup>, stacking a few Watson-Crick base pairs above and below a given base pair modifies its NMR spectroscopic parameters by an experimentally measurable amount (results from vacuum studies). However, in addition to a suitable level of theory, the reliable calculation of NMR parameters requires the inclusion of solvent effects.<sup>16</sup>

The structure and function of biomolecules are strongly influenced by their hydration layers<sup>17–19</sup>, which consist of a dynamic network of water molecules.<sup>20</sup> The effect of solvent is caused by the interaction of solvent molecules with the solute -enthalpic component- and by the hydrophobic effect, which is mainly entropy driven at room temperature.<sup>21–23</sup>

The layer of water molecules surrounding a double-stranded DNA molecule plays an essential role in preserving its structure and proper biochemical function.<sup>24,25</sup> The interactions of DNA chains with small molecules and proteins are mediated by the solvent structure, which forms an activation barrier for essential biological processes, including DNA transcription, which involves biomolecules that bind to DNA shifting the solvation layer.<sup>26–28</sup> Therefore, the water network that underlies the solvent structure is an essential ingredient in the biological architecture,<sup>17</sup> whose effects can not be introduced only from average effects on the mentioned functions.

Regarding the theoretical studies of DNA with water molecules, we can find: i) those designed to determine the dynamics of water molecules in the vicinity of DNA, carried out by classical methods; ii) those aimed to assess the effects of the solvent on the electronic structure of DNA, by means of quantum chemistry methods. In the first case, molecular dynamics (MD) simulations recently showed that there is a wide range of dynamics of water molecules, and molecules with very low mobility were identified in the minor groove of DNA, which is consistent with observations made through X-ray.<sup>29</sup> In the second case, it was found that there is a great dependence of DNA replication with  $\pi$ -stacking and the presence of water as solvent.<sup>30–33</sup> These works detail the importance of the role played by HBs, angles of twist and stacking interactions in the stability of complementary and non-complementary base pairs. Similar works were recently carried out to study the stability of canonical and noncanonical DNA base pairs.<sup>34–37</sup>

In recent years some systematic works were developed to rationalize and understand the relationship between the crystal structures with the NMR chemical shift tensors.<sup>8,38</sup> There were also published the implementation of a new method for the evaluation of NMR chemical shifts of large biomolecules.<sup>39</sup> In this study we introduce different theoretical ways to evaluate the effects and importance of solvent and non-covalent interactions, such as hydrogen bonds and  $\pi$ -stacking, on NMR magnetic shieldings of small DNA fragments. We used different models to include solvent effects in systems that contain more than one pair of ni-

trogenous bases; that is, a reduced number of pairs stacked above and below a central pair, which is taken as witness of the changes that the magnetic parameters undergo when increasing the size of the DNA fragment.

## 2 Theoretical models

We shall outline here the theoretical models that were used to study solvent and stacking effects. Those effects are treated as being independent one to the other or as joint effects.

### 2.1 Solvation models

In most cases, solvent effects on NMR calculations are accounted for by using the Tomasi integral equation formalism - polarizable continuum model (IEF-PCM) scheme or simply PCM.<sup>40–42</sup> The continuous model procedure has a solid theoretical basis, and it is the most used today, mainly due to its simplicity and the small computational cost required. The effect of the solvent is simulated as an apparent charge distribution dispersion on the surface of the cavity (in which the molecule of interest is located). Thus, when solvent effects are calculated within the PCM scheme short-range specific solvation effects are included in an average form. In this way this model works quite well when some specific solute-solvent intermolecular interactions do not play a relevant role. On the other hand, the explicit representation of the solvent provides a detailed description of the solvent-solute interaction. However, because the number of solvent molecules must be large enough to provide at least several layers of solvation, the use of an implicit solvent introduce solvent average effects at lower computational cost.

In some cases it is also possible to perform a *combination of both methods for including solvent effects*. Here the explicit solute-solvent system, *i.e.* the molecule of interest together with the explicit solvent molecules, is introduced in the cavity formed by the implicit solvent model. In this way, the explicit interactions between solute and solvent are considered, while making use of the computational advantages of the continuous solvent model.<sup>43–45</sup>

On the other hand, given that discrete methods accounts for hydrogen-bonds explicitly and, thus, they are more suitable to use when particular HBs of the solvent shall be taken into account, two layers of water molecules were added to the dodecamer structure. Subsequently, their positions were optimized by means of MD simulations at different times relaxing afterwards the structure of the dodecamer.

Taking all this into account, three procedures were considered: a) explicit solvent; b) implicit solvent (polarizable continuum model, PCM) and c) explicit in addition to implicit solvent.

### 2.2 DNA fragments and their water network

We have chosen a large enough DNA fragment obtained from the *Protein Data Bank* (PDB ID: 1BNA) which corresponds to the crystal structure of a B-DNA double-stranded dodecamer. Its nucleotide sequence is the following: 5'd (CGCGAATTCGCG) 3'.

In order to make feasible its treatment with state of the art theoretical models, the phosphate and sugar chains were replaced by methyl groups. This replacement simulate steric effects produced

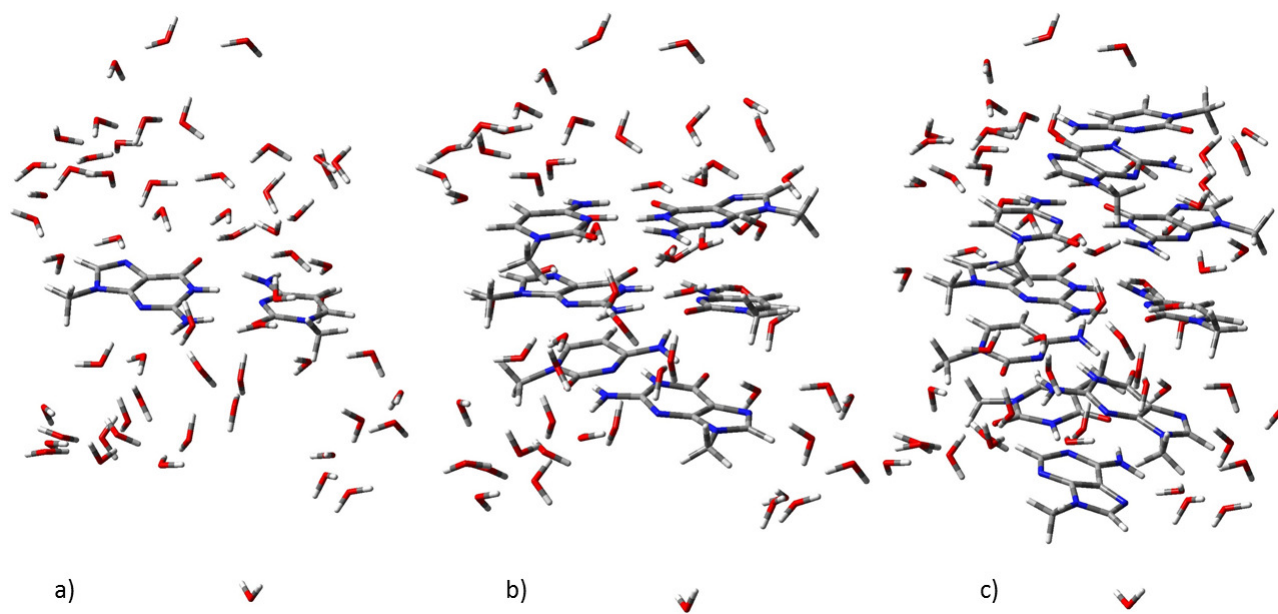


**Fig. 1** Construction of explicit fragments. a) F1, b) F3 and c) F5, with explicit water molecules. Note that in the first case the base pair 3 is isolated (F1), then it is in the center of the GCG sequence (F3) and finally in the center of the CGCGA sequence (F5), being the solvation network the same for all three cases.

by the groups they replace having no impact in the computational cost. The rest of the geometric structure of the dodecamer remains unchanged.

To justify the replacement of phosphate and sugar chains by methyl groups we assumed that the water network model corresponded to the water molecules which were located in the minor and major grooves limited by the backbone of sugars and phosphates of the DNA chain, being the addition of methyl groups a valid strategy to ensure that water molecules maintain their position. Several studies have shown that, in addition to being the ones with the least mobility with respect to bulk waters,<sup>29,46</sup> these solvent molecules are the ones with the greatest interaction and influence on the properties and function of DNA.

The largest fragment we have chosen to carry out these series of studies was extracted from the dodecamer and has the sequence CGCGA (when the base pairs are numbered, their numbers are 12345). Since our interest is focused on a single pair as witness of the inner electronic behavior in a given fragment, we selected the central pair (number 3, see Figure 2a). This same pair will be considered as the for sequences containing three and five base pairs, since the smallest sequence (three base pairs) is drawn from the center of the five base pair fragment. Thus, the GCG sequence corresponds to the 234 pairs. To simplify the identification of these three fragments, we used the following notation:

- **F1:** pair 3 (the witness pair) is isolated;
- **F3:** pair 3 is in the center of the sequence of three GCG pairs;
- **F5:** pair 3 is in the center of the sequence of five CGCGA pairs.

In order to simulate the effects of the explicit solvent consistently, we considered a “solvation network” for the fragment of five base

pairs (F5) and then, the same network in all the other cases. This means, the same “solvation network” was used to simulate explicit solvent effects on fragments F5, F3 and F1.

Once these three basic structures were defined, we introduced the following solvent models:

- **VAC:** Vacuum (no water molecules included).
- **ES:** Explicit solvent: a network of water molecules corresponding to two solvation layers (60 water molecules, maintaining the same network for F1, F3 and F5), as represented in Figure 1.
- **IS:** Implicit solvent (PCM).
- **ES + IS:** Explicit solvent plus implicit solvent: a network of water molecules corresponding to the two solvation layers (60 water molecules, maintaining the same network for F1, F3 and F5), combined with the inclusion of the implicit solvent (PCM).

The NMR magnetic shieldings of the special pair 3 were then studied for the fragments F1, F3 and F5 combined with the solvent models described above.

### 3 Computational details

The geometry of the methyl groups replacing the phosphate and sugar groups in the dodecamer, and the positions of the solvent molecules of water were optimized using MD. As stated above, in macromolecular systems, the first two solvation shells from the molecular surface were found to be more ordered than bulk, especially in polar systems such as DNA<sup>29,46,47</sup>. Indeed, it is seen that the first solvation layer, which is critical for the QM calculations, remains stable in terms of hydrogen bonding to the bases

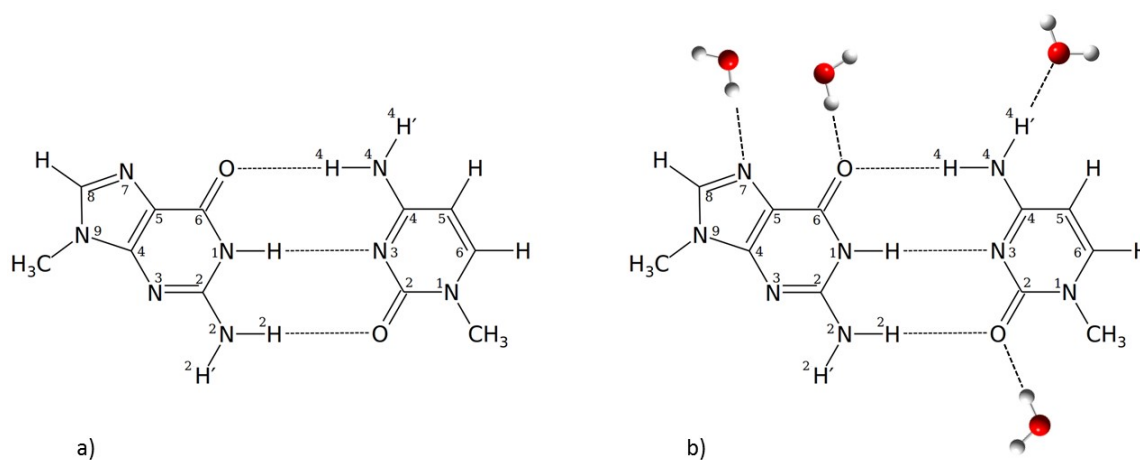


Fig. 2 Structure of the witness pair. a) Isolated guanine-cytosine pair and b) Water molecules surrounding the GC pair in the explicit solvent model.

throughout the MD simulation, so similar results should be obtained regardless the chosen snapshot. To illustrate this point, in Figure 3 we show the distance of the water molecules to the corresponding heteroatoms in the witness pair (cf. Fig. 2) plotted along the simulation. The water molecules remain within 2.5 Å of the witness pair during over 95% of the simulation in the case of the HBs formed between the water molecule and the corresponding N or O atoms in the pair, whereas this value is closer to 85% for the NH group, in all cases indicating a stable interaction. Taking this into account, and to capture the effect of explicit solvent in calculating chemical shifts, a representative snapshot including all the HBs referred above was selected from the end of the production stage. Afterwards, the different fragments of interest were obtained.

The main contribution to the interaction energy comes from the dispersion contribution,<sup>48</sup> which indicates that electron correlation corrections should be included in the calculation of the arene-arene interaction. Different efforts to overcome the inability of density functional theory (DFT) to explain dispersion were discussed by Grimme *et al.*<sup>49</sup> On the other hand, Grimme,<sup>50</sup> described some characteristics of the interactions between parallel stacks of arenes. He found that genuine  $\pi - \pi$  interactions are only at work for short intermolecular interactions, and that they are caused by specific electron correlation. For systems with a number of carbon atoms that is less or equal to 10 there is little theoretical evidence that  $\pi$  orbitals play a special role. Therefore, the term “ $\pi - \pi$  stacking” should be used as a convenient structural descriptor for the mode of interaction in unsaturated molecules.

These are the reasons why magnetic shielding calculations were carried out here at the DFT level and both, London orbitals and GIAO (*gauge-including atomic orbitals*) orbitals in order to guarantee the independence of the results with respect to the origin of the gauge.<sup>51–53</sup> Furthermore, the functional B97-D<sup>54</sup> (which includes dispersion correction effects) and the set of Gaussian bases 6-311++G\*\*<sup>55</sup> were used as a trade-off between accuracy and computational cost. Calculation of shieldings, as well as the inclusion of Tomasi’s polarizable continuum model (PCM)

were performed with the Dalton2016 program package.<sup>56</sup>

### 3.1 Molecular dynamics simulations

Molecular dynamics (MD) simulations were performed using GROMACS v5.1 package<sup>57</sup> using the Amber94 force field for the nucleic acid<sup>58</sup>. The system was solvated with the SPCE water model in a triclinic box, extending 10 Å from the DNA dodecamer, and neutralized adding sufficient NaCl counter ions to reach 0.15 M concentration. Bond lengths were constrained using the LINCS algorithm<sup>59</sup> allowing a 2 fs time-step. Long-range electrostatics interactions were taken into account using the particle-mesh Ewald (PME) approach. The non-bonded cut-off for Coulomb and Van der Waals interactions were both 10 Å, and the non-bonded pair list was updated every 25 fs. Energy minimization was conducted through the steepest-descent algorithm, until the maximum force decayed to 1,000 kJ/mol•nm. Then an equilibration of the whole system was performed by 500 ps of NVT simulation followed by 500 ps of NPT simulation. Temperature was kept constant at 300 K using a modified Berendsen thermostat<sup>60</sup> with a coupling constant of 0.1 ps. Constant pressure of 1 bar was applied in all directions with a coupling constant of 2.0 ps and a compressibility of  $4.5 \cdot 10^{-5} \text{ bar}^{-1}$ . After the equilibration, a 5 ns production was carried out and different structures/snapshots were saved along this trajectory.

## 4 Results

Magnetic shieldings of selected atoms that belong to the guanine-cytosine witness pair (pair 3) are given in Table S1 of the Supplementary Information. As observed, our theoretical results are close to the experimental ones for the shielding of most of the atoms studied. Regarding the accuracy obtained with the different theoretical solvent models used in this work, we show in Figures 4 and 5 the RMSD and MAE values obtained from the differences among theoretical calculations and experimental measurements. It is observed that the F5-ES model is the most accurate even though trends are different in both parameters.

In order to get a more direct knowledge of the pattern of de-

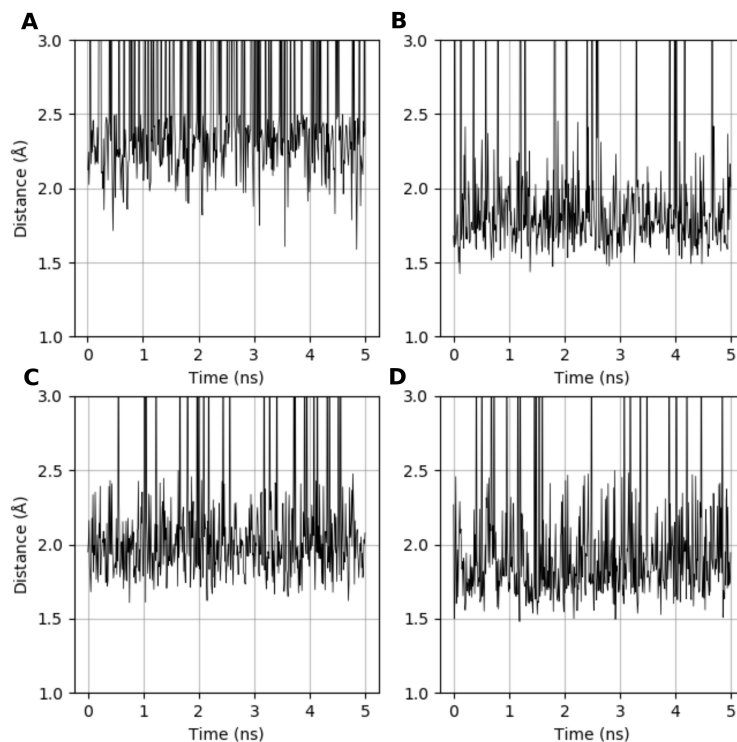


**Fig. 3** Water - witness pair distance along the MD simulation for the external HB interactions presented in Figure 2. The distances between (A) the oxygen atom of a water molecule and the NH group in position 4 of the cytosine base, (B) the hydrogen atom of a water molecule and the oxygen atom in the carbonyl group of the cytosine base, (C) the hydrogen atom of a water molecule and the nitrogen atom in position 7 of the guanidine base, and (D) the hydrogen atom of a water molecule and the oxygen atom in the carbonyl group of the guanidine base are plotted against time.

pendence of the shieldings with both effects, solvent and stacking as they are described with our theoretical models, we shall use and analyze Figures 7, 8 and 6 (numerical values are taken from Table S1).

#### 4.1 Solvent effects from the ES model

Initially, we analyze in detail the behavior of the shieldings with the ES solvent model, taking as the comparative parameters the values of shieldings in fragments without solvent (VAC model). Then we consider briefly the other two solvent models used.

As expected, the presence of the solvent modifies the calculated magnetic shieldings in vacuum (for the three fragments studied here), specially for the shieldings of C<sub>2</sub>-G, C<sub>6</sub>-G and H<sub>2</sub>-G, and C<sub>4</sub>-C, H<sub>4</sub>-C and N<sub>3</sub>-C.

##### 4.1.1 Shieldings of carbon atoms

There are two carbons that are more involved in the coupled effects of solvent and stacking. They belong to those substructures of the Guanine and Cytosine that are connected each other through HBs. In fact those carbons are also close to few water molecules that are bonded to oxygens and NH through HBs.

In guanine the combined effect is observed in the shielding of C<sub>2</sub>-G and C<sub>6</sub>-G carbons in the fragment F3. The variations are

in total of -4 ppm and 1.7 ppm, respectively. In the case of the shielding of C<sub>2</sub>-G in vacuum, the stacking produces a deshielding that is highly enhanced when the solvent effect is added. On the other hand, in Cytosine the combined effect becomes important for C<sub>2</sub>-C and C<sub>4</sub>-C when the fragment F3 is replaced by the fragment F5. This is due to the fact that the dependence of the stacking with the solvent follows a different trend: while in VAC a shielding trend is observed when going from fragment F3 to fragment F5, in the ES model such a trend is opposite. For example, the shielding of C<sub>4</sub>-C increase in VAC almost 1 ppm away, it decrease in ES more than 1 ppm.

##### 4.1.2 Shieldings of nitrogen atoms

For nitrogen N<sub>1</sub>-G (Figure 7), solvent effects are weak in all three F-type fragments simultaneously. It is less than 1 %. This situation is also observed for other atoms, though not in the three fragments simultaneously. In the case of N<sub>1</sub>-G stacking effects and solvent effects are both very small. This is not the case for the shielding of H<sub>2</sub>-G which is not affected by the presence of the solvent in F1 and F5, but it undergoes a shielding change at F3 (see Figure 8). The hydrogen atoms, H<sub>2</sub>-G and H<sub>4</sub>-C are weakly equivalent about their neighbor atoms and bondings, but trends of their shielding behavior for fragments F1, F3 and F5 in VAC

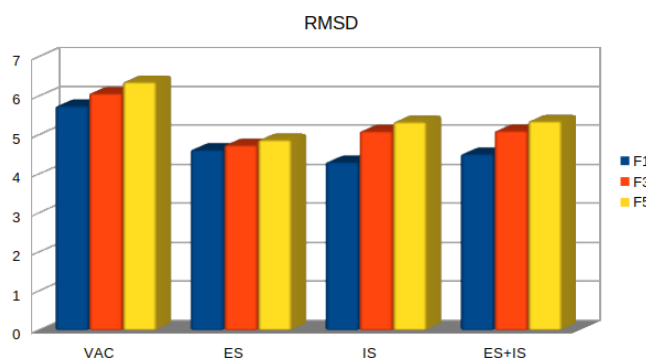


**Fig. 4** Results of the Root Mean Square Deviation, RMSD, values (in ppm) taken between the calculated and experimental chemical shifts for all four models used in this study (VAC, ES, IS, ES+IS).

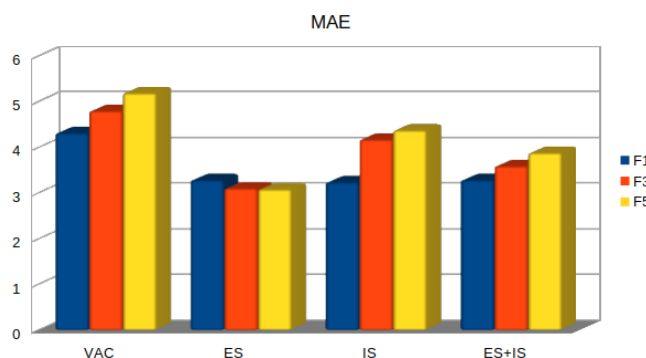


**Fig. 5** Results of the Mean Absolute Error, MAE, values (in ppm) taken between the calculated and experimental chemical shifts for all four models used in this study (VAC, ES, IS, ES+IS).

are opposite. Such a behavior needs more studies for getting a reliable explanation.

On the other hand, it is worth to mention that, in all cases, the presence of the solvent modifies the stacking effect, though for some atoms this influence is small. In these cases, the solvent effect modifies the values of the shieldings but not their dependence with the stacking effect. The most external nitrogens (*i.e.* N<sub>2</sub>-G and N<sub>4</sub>-C) follows this behavior. They are highly exposed to interactions with nearby water molecules and so, they become deshielded, even though stacking effects produces an opposite effect. The nitrogen N<sub>2</sub>-G is more deshielded when we go from F1 to F5, but the nitrogen N<sub>4</sub>-C is more shielded. Furthermore, given that in our ES model the Hydrogen H<sub>4</sub>-C has an explicit Hydrogen bonding with one of the water molecules, this fact can explain the higher solvent effect on the nitrogen N<sub>4</sub>-C (10 ppm) than that on the nitrogen N<sub>2</sub>-G (5 ppm). For the nitrogen N<sub>7</sub>-G its explicit bonding with a water molecule produced a shielding on it (for F5-VAC its chemical shift is 250.68 ppm and for F5-ES it is 234.88 ppm), and so, it becomes closer to the experimental value, which is 238 ppm. This is in line with previous interpretations that relate the involvement of the free electron pair of the nitrogen atom (N<sub>7</sub>) in the hydrogen bonding, which results in a less effective paramagnetic deshielding and so, reducing its chemical shift.<sup>61</sup>

In the case of the nitrogen atoms that are not close to the molecular surface of solute molecules, one may expect that their shielding dependence with the presence of solvent would be smaller than such a dependence of the more external ones. As can be observed in Figure 7, this is what happens for the shielding of nitrogen N<sub>1</sub>-G, whose behavior in vacuum is similar to that of nitrogen N<sub>3</sub>-C. In this last case the total effect (solvent plus stacking) produce a variation of +8 ppm (positive or negative signs will be used here to indicate shielding or deshielding effect, respectively).

#### 4.1.3 Shieldings of hydrogen atoms

The shieldings of hydrogen atoms have the same trends as those of the nitrogen atoms to which they are bounded when solvent and stacking effects are included. Solvent effects produce changes that are of different magnitudes. In the case of H<sub>4</sub>-C the change is around -3.3 ppm, and for H<sub>2</sub>-G around -1 ppm. Those hydrogen atoms are the most affected by the influence of water molecules (those values arises when comparing ES with VAC in the three fragments). On the contrary, H<sub>1</sub>-G, H<sub>2</sub>-G and H<sub>4</sub>-C, which in the vacuum model already form intermolecular HBs are more shielded in the presence of the solvent. Thus, while N<sub>2</sub>-G and N<sub>4</sub>-C are deshielded by the presence of the solvent, the hydrogen atoms, H<sub>2</sub>-G and H<sub>4</sub>-C, attached to them are more shielded.

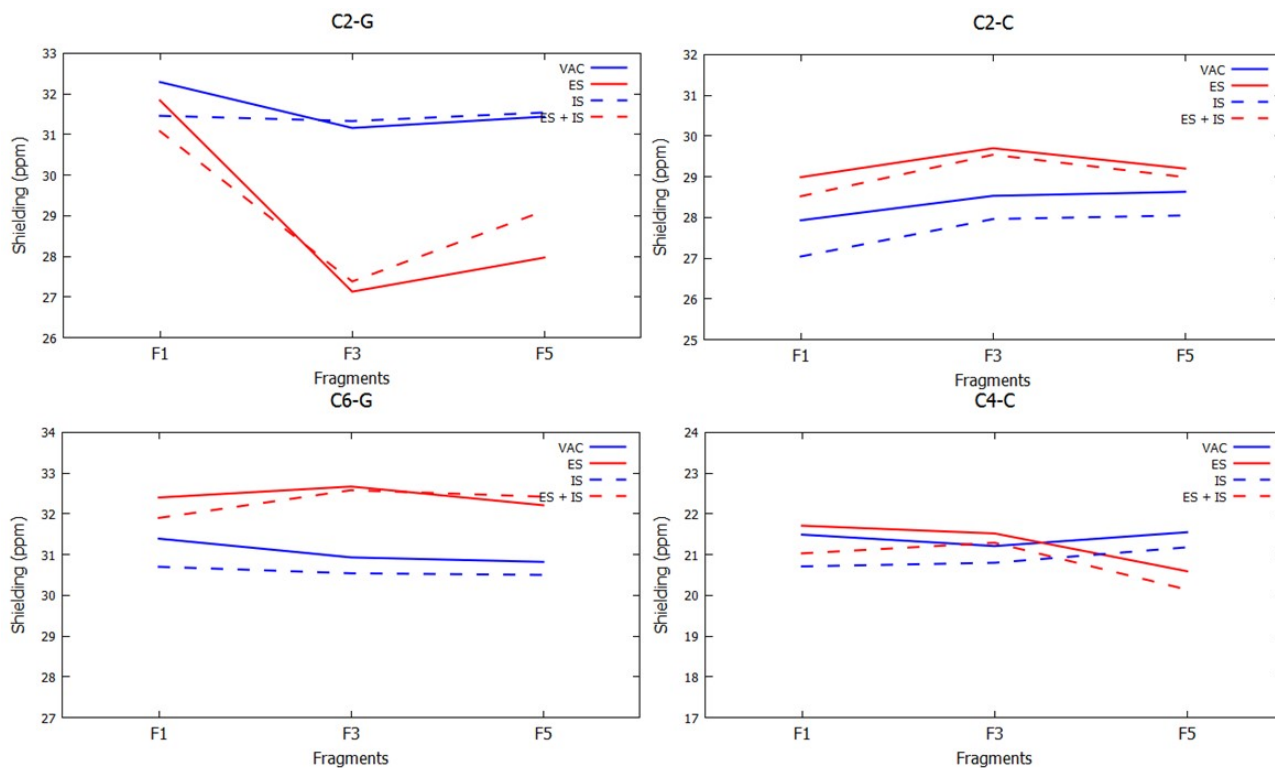


**Fig. 6** Behavior of  $^{13}\text{C}$  shieldings GC (base pair 3): in vacuum (VAC), with explicit solvent (ES), with implicit solvent (IS) and explicit and implicit solvent (ES + IS).

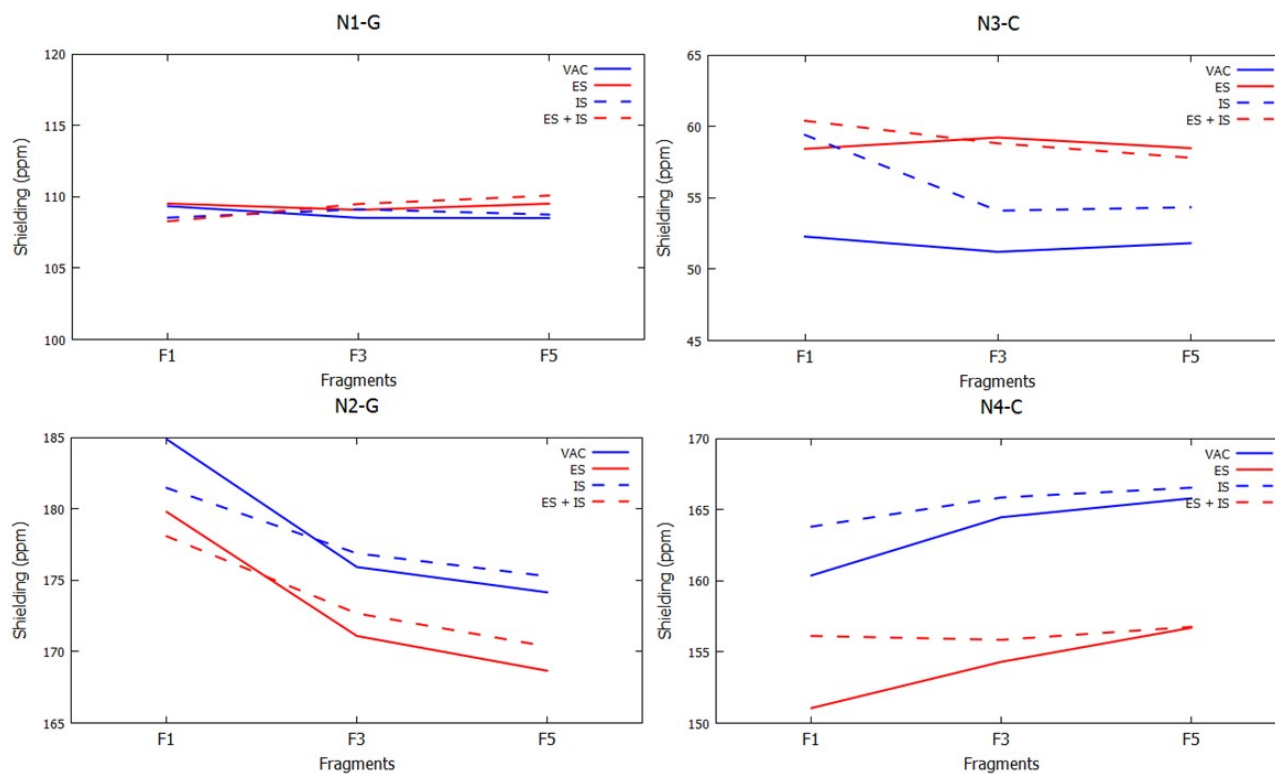


**Fig. 7** Behavior of  $^{15}\text{N}$  magnetic shieldings in GC (base pair 3): in (VAC), with explicit solvent (ES), with implicit solvent (IS) and explicit and implicit solvent (ES + IS).



We then realize that the behavior of the most external nitrogen atoms are closely related with the behavior of hydrogens H<sub>2</sub>-G and H<sub>4</sub>-C.

In the case of hydrogens H<sub>2</sub>-G and H<sub>4</sub>-C, we observe that they have the indirect influence of two HBs. One arises due to the H<sub>4</sub> ... OH<sub>2</sub> HB. Such HB modifies  $\sigma(\text{H}'_4)$  in about 4 ppm (deshielding). For all those  $\sigma(\text{H})$ , meaning  $\sigma(\text{H}_4\text{-C})$ ,  $\sigma(\text{H}'_4\text{-C})$  and  $\sigma(\text{H}_2\text{-G})$  the trend of stacking effects are positive (meaning that the shieldings increase with stacking). On the other hand, ES effects do affect more  $\sigma(\text{H}'_4\text{-C})$  and  $\sigma(\text{H}_4\text{-C})$ . This is due to the explicit formation of HB involving H<sub>4</sub>.

## 4.2 The non ES solvent models

In Figures 7, 8 and 6 we observe that, in the case of the implicit model, and considering the variations between fragments F3 and F5, the shieldings do follow the same behavior as that of the shieldings in the vacuum model in all cases.

A similar correspondence with the ES model is observed for the third model, ES + IS, when we compare the behavior of shieldings between fragments F3 and F5, but this does not happens in all cases (N<sub>4</sub>-C and H<sub>4</sub>-C). This mixing solvent model represents an increase of around 25 % in the time of calculations with respect to the use of the explicit model for the F5 fragment. Therefore, the explicit model is the best option as long as one is able to select a good number of water molecules and correctly model the spatial arrangement of them. This finding is closely related with previous ones in which the calculations were performed on the experimental structure and on the snapshots of the molecular dynamic simulation.<sup>62–64</sup>

When the PCM model is applied on the F1 fragment the solvent effect on the witness pair is not correct. In this case F1 is completely “surrounded by the solvent” which must not be the case. So, we should only consider as valid, results of calculations with the implicit model on fragments F3 and F5. A similar situation does occurs for the ES + IS model.

## 5 Discussion

In this section we want to highlight some clear patterns that appear in our studies. We start with carbon shieldings, followed by nitrogens and hydrogens.

Most of previous studies have been focused on describing trends of carbon <sup>13</sup>C shieldings due to hydrogen-bonding formation and stacking effects,<sup>8,65</sup> though the considered HBs are only those arising from the formation of Watson-Crick hydrogen bonds. Instead we are involved in describing trends of shieldings due to the presence of solvent molecules that can eventually form HBs with atoms belonging to the borders of Guanine or Cytosine.

For purine-based compounds it is known that <sup>13</sup>C chemical shift tensors are sensitive to local structural changes like a substitution in the purine ring, tautomerism, and intermolecular interactions<sup>66</sup>. They can be influenced by the interactions of neighboring nitrogens with other molecules. Furthermore, in Ref. 65 it was shown that base stacking tends to shield base carbons and Watson-Crick hydrogen bond formation usually deshields carbons near certain of the HBs donor and acceptor heteroatoms. It may

happens then that shielding and deshielding effects cancel each other at some locations, but a substantial net deshielding effect at a particular carbon nucleus appears to be diagnostic of a Watson-Crick HB formation at a nearby site like what happens to carbon C<sub>2</sub>-G. The hydrogen-bonding and stacking interactions may add to or subtract from one another to produce total values observed experimentally.<sup>8</sup>

In Figure 2b) we show which heteroatoms of the witness pair are engaged in external HBs. The carbons that are bonded to them are C<sub>2</sub>-C, C<sub>4</sub>-C and C<sub>6</sub>-G and they are more shielded with respect to their values in vacuum. Furthermore, when the F5 fragment is considered in the ES model the trend observed due to stacking is that of an smooth deshielding.

Following a similar reasoning, the carbon C<sub>2</sub>-G is bounded to both N<sub>2</sub>-G and N<sub>3</sub>-G, which are not engaged in explicit HBs with water molecules. We observe that carbon C<sub>2</sub>-G is highly deshielded in ES as compared to VAC, but it becomes little shielded when going from fragment F3 to F5 as we should expect from previous findings of stacking effects.<sup>65</sup>

Let us now focus our analysis on two NH<sub>2</sub> groups which have equivalent positions in the central GC pair, meaning N<sub>2</sub>H<sub>2</sub> of guanine and N<sub>4</sub>H<sub>4</sub> of cytosine. They both have external hydrogen atoms that could interact with solvent molecules of water. They both also have one hydrogen atom that belongs to a HB between guanine and cytosine, meaning N<sub>2</sub>-H<sub>2</sub> ... O<sub>2</sub> and N<sub>4</sub>-H<sub>4</sub> ... O<sub>6</sub>. The NH<sub>2</sub> group that belongs to cytosine has an explicit HB with a water molecule, though the other NH<sub>2</sub> group does not have such an explicit H-bond.

For both NH<sub>2</sub> groups the behavior of the shieldings of each pair of equivalent atoms is quite similar (but with different absolute values). As observed in Table 1 of SI, the total effects for the external hydrogen atoms are such that they are both deshielded. The hydrogen of cytosine (H<sub>4</sub>-C) is more deshielded than its equivalent in guanine (H<sub>2</sub>-G), being its values -3.3 ppm and -1 ppm, respectively, taken as the difference among F5-VAC and F5-ES models. Both nitrogen atoms are also deshielded (9.1 ppm for N<sub>4</sub>-C vs 5.5 ppm for N<sub>2</sub>-G). On the other hand the hydrogen atoms that belongs to the HBs between cytosine and guanine are both more shielded (0.5 ppm for H<sub>4</sub>-C vs 0.1 ppm for H<sub>2</sub>-G). This means that the N-H bond that interacts with the solvent is highly affected by it as compared with the one that does not have a HB with solvents. Those interactions modifies the electronic distribution and thus, the magnetic shieldings.<sup>38</sup>

We discuss now the changes that the solvent may produces on the trends of stacking effects, which can only be observed by considering the fragments F3 and F5. One of the most interesting cases is the shielding of C<sub>4</sub>-C. When there is no solvent the stacking effects is such that that carbon is shielded but when solvent is included the carbon is deshielded.

There are some atoms for which solvent effects have different signs with respect to the stacking effects in the sequence F1 → F3 but then the converge from F3 → F5. Few clear examples are N<sub>3</sub>-C, H<sub>2</sub>-G, C<sub>6</sub>-G. It seems that when the fragment F5 is taken into account the total effect becomes again similar to what happens for the F1 fragment. In all cases there is a net shielding effect.

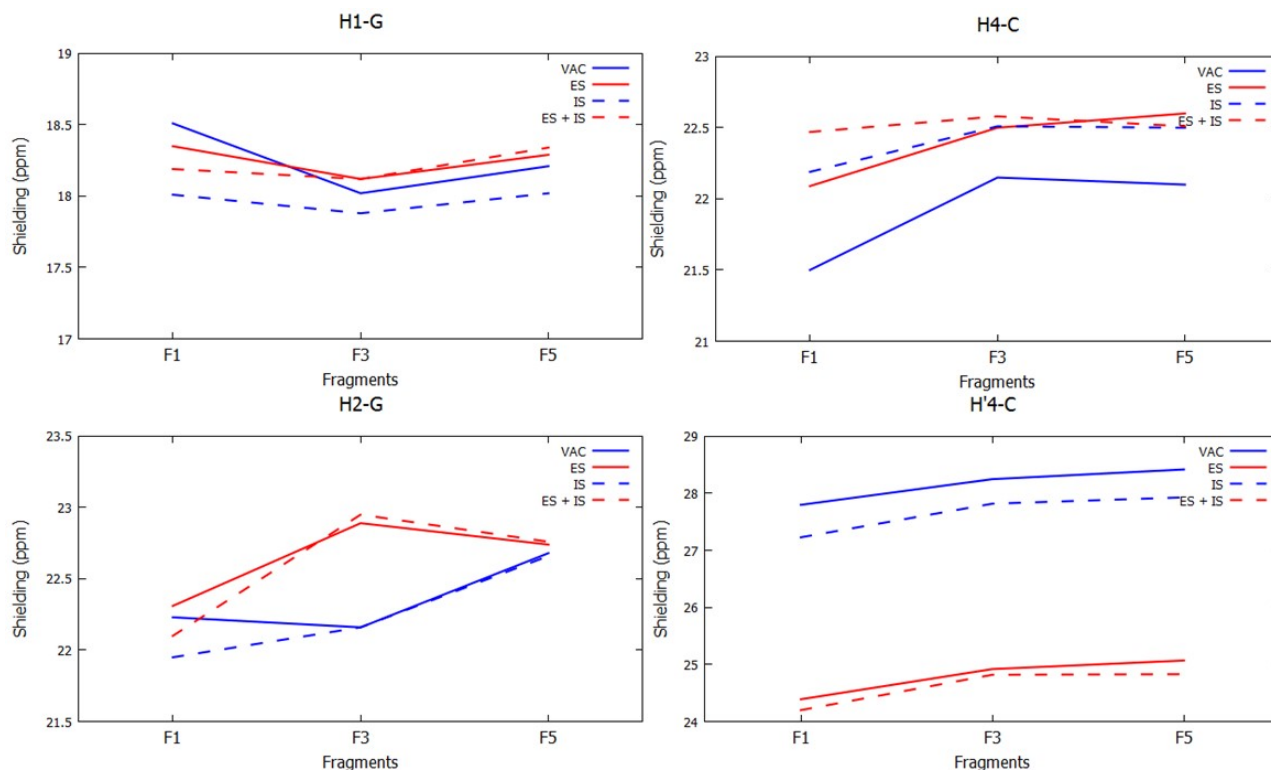


**Fig. 8** Behavior of  $^1\text{H}$  shieldings in GC (base pair 3): in vacuum (VAC), with explicit solvent (ES), implicit solvent (IS) and explicit and implicit solvent (ES + IS).

## 6 Conclusions

In a previous work we have studied the likely existence of long-range transmission of intra-molecular interactions in small fragments of molecules of DNA that could influence the behavior of response properties.<sup>15</sup> To check this hypothesis we applied a simple theoretical model which only included the  $\pi$ -stacking and guanine-cytosine HBs effects on the NMR shielding. We have considered the shielding of the atoms belonging to the central dimer of a Watson-Crick chain as special sensors of the influence of that interactions.

To fulfil that requirement, we developed a novel scheme that consisted in considering trends of shieldings of atoms belonging to a central base-pair, like GC, of a small DNA fragment when the number of base-pairs is increased from both, above and below of that central base-pair. The helical layers were taken from the Protein Data Bank. In order to make its treatment feasible we take out all sugars and phosphate groups, and replaced them by methyl groups. The geometrical structure of each DNA base-pairs was then not modified. We first applied this scheme to selected fragments in vacuo and now, as a second step, we include the treatment of solvent effects. Different solvent models were introduced: a) explicit solvent with two solvation layers (ES), b) implicit solvent using PCM and c) a mix of both. As in the previous work the central pair in the DNA fragment which contains one (F1), three (F3) or five (F5) pairs was taken as the one which witnesses the changes the magnetic parameters undergo when the size of the DNA fragment is increased and the solvent model

is included.

Results of calculations with our more accurate theoretical model, the F5-ES one, were confronted with available experimental measurements. We found a good matching using the B97-D/6-311++G\*\* level of theory, showing that the F5-ES model is reliable enough to analyze the influence of the two main electronic effects involved in fragments of DNA molecules (meaning  $\pi$ -stacking and solvent) on magnetic response properties.

Our results follow well defined patterns, being some of them in line with previous findings, while others add new insights. When the implicit solvent model is considered, results closely resemble those results found using the vacuum model. Instead, new trends appear when the explicit solvent model, ES, is considered. Such ES model has a network of water molecules that is composed of two solvation layers.

Among the new findings we should mention that:

- when the water network is included, the shielding of individual atoms of equivalent groups, like the  $\text{NH}_2$ , follows a similar trend (deshielding the N – H pair of atoms)<sup>67</sup>, though the stacking effect can have an opposite trend. The net effect is deshielding;
- there is deshielding of the atoms that belong to the external N–H bonds that are in contact with the solvent.<sup>67</sup> Such a behavior is highly enhanced by the solvent network, as observed for H'4-C, whose magnetic shielding is reduced in more than 10%. In the same manner, the nitrogen atom N4-C is deshielded by a similar amount;

- the atoms belonging to external N–H bonds, which are also in contact with the solvent but are not part of HBs with water molecules, are also deshielded but in by a lesser amount;
- carbon atoms that belongs to C=O bonds for which the oxygen has a HB with a solvent water molecule, like C<sub>2</sub>-C and C<sub>6</sub>-G, are shielded;
- in the case of the atoms that belongs to a given HB between guanine and cytosine, say (N<sub>1</sub>-H<sub>1</sub> ... N<sub>3</sub>), the influence of the explicit solvent of water molecules is much higher on the shielding of the acceptor nitrogen atom (nitrogen of cytosine) than the donor, being its effect around 10% against 1%. In both cases there is a deshielding effect,
- in the case of hydrogen atoms that belong to HBs between guanine and cytosine, as happens for H<sub>1</sub>-G, they are little more shielded in the presence of the solvent, meaning that solvent effects can even influence the shielding of those hydrogen atoms. This is in line with previous publications,<sup>31,68</sup>;
- carbon atoms that have as neighbors two nitrogen atoms, one of which belongs to external N – H bonds, like C<sub>2</sub>-G and C<sub>4</sub>-C, are deshielded due to solvent effects.

We have also found some other cases (N<sub>3</sub>-C, H<sub>2</sub>-G and C<sub>6</sub>-G) for which solvent effects change the behavior of the stacking as observed in vacuum. The largest changes appear for the fragment F3 but these changes are again modified when the fragment F5 is involved. Then, when the number of base pairs is increased (which enhance the  $\pi$ -stacking effect) there are changes on the electronic structure that may modify in an important manner the behavior of the shieldings in the central base pair.

In order to get converged results to compared with experimental measurements we are working at the moment to include more pairs, such as fragments as long as F7 and even F9.

## Author Contributions

We strongly encourage authors to include author contributions and recommend using CRediT for standardised contribution descriptions. Please refer to our general author guidelines for more information about authorship.

## Conflicts of interest

There are no conflicts to declare.

## Acknowledgements

The authors gratefully acknowledge support from the National Research Council for Science and Technology (grants PIP 112-20130100361) and the Argentinian Agency for Promotion of Science and Technology (ANPCYT, grant PICT 2016-2936 to GAA and PICT 2017-3767 to CNC).

## Notes and references

- 1 E. A. Meyer, R. K. Castellano and F. Diederich, *Angew. Chem. Internat. Edit.*, 2003, **42**, 1210–1250.

- 2 S. Yanagisawa, P. B. Crowley, S. J. Firbank, A. T. Lawler, D. M. Hunter, W. McFarlane, C. Li, T. Kohzuma, M. J. Banfield and C. Dennison, *J. Am. Chem. Soc.*, 2008, **130**, 15420–15428.
- 3 V. L. Malinovskii, F. Samain and R. Häner, *Angew. Chem.*, 2007, **119**, 4548–4551.
- 4 R. Fasan, R. L. A. Dias, K. Moehle, O. Zerbe, D. Obrecht, P. R. E. Mittl, M. G. Grütter and J. A. Robinson, *ChemBioChem*, 2006, **7**, 515–526.
- 5 C. A. Hunter and J. K. M. Sanders, *J. Am. Chem. Soc.*, 1990, **112**, 5525–5534.
- 6 C. A. Hunter, K. R. Lawson, J. Perkins and C. J. Urch, *J. Chem. Soc., Perkin Trans. 2*, 2001, 651–669.
- 7 P. L. Bora, M. Novák, J. Novotný, C. Foroutan-Nejad and R. Marek, *Chemistry—A European Journal*, 2017, **23**, 7315–7323.
- 8 K. Bouzková, M. Babinský, L. Novosadová and R. Marek, *Journal of Chemical Theory and Computation*, 2013, **9**, 2629–2638.
- 9 C. Foroutan-Nejad, Z. Badri and R. Marek, *Physical Chemistry Chemical Physics*, 2015, **17**, 30670–30679.
- 10 J. Novotný, S. Bazzi, R. Marek and J. Kozelka, *Physical Chemistry Chemical Physics*, 2016, **18**, 19472–19481.
- 11 V. M. Anisimov, A. Ziemys, S. Kizhake, Z. Yuan, A. Natarajan and C. N. Cavasotto, *J. Comput. Aided Mol. Des.*, 2011, **25**, 1071–1084.
- 12 V. M. Anisimov, V. L. Bugaenko and C. N. Cavasotto, *ChemPhysChem*, 2009, **10**, 3194–3200.
- 13 C. N. Cavasotto and M. G. Aucar, *Frontiers in Chemistry*, 2020, **8**, 246.
- 14 M. Dračinský and R. Pohl, in *M. Dračinský and R. Pohl*, Elsevier, 2014, vol. 82, pp. 59–113.
- 15 F. A. Martínez and G. A. Aucar, *Physical Chemistry Chemical Physics*, 2017, **19**, 27817–27827.
- 16 K. J. Jose and K. Raghavachari, *Journal of chemical theory and computation*, 2017, **13**, 1147–1158.
- 17 P. Ball, *Chem. Rev.*, 2008, **108**, 74–108.
- 18 Y. Levy and J. N. Onuchic, *Annu. Rev. Biophys. Biomol. Struct.*, 2006, **35**, 389–415.
- 19 L. J. Rothschild and R. L. Mancinelli, *Nature*, 2001, **409**, 1092.
- 20 H. J. Bakker and J. L. Skinner, *Chem. Rev.*, 2009, **110**, 1498–1517.
- 21 E. Arunan, G. R. Desiraju, R. A. Klein, J. Sadlej, S. Scheiner, I. Alkorta, D. C. Clary, R. H. Crabtree, J. J. Dannenberg, P. Hobza *et al.*, *Pure and Applied Chemistry*, 2011, **83**, 1619–1636.
- 22 M. Dračinský and P. Bour, *J. Chem. Theory Comput.*, 2009, **6**, 288–299.
- 23 M. Dračinský, J. Kaminský and P. Bour, *J. Phys. Chem. B*, 2009, **113**, 14698–14707.
- 24 C. T. Middleton, K. de La Harpe, C. Su, Y. K. Law, C. E. Crespo-Hernández and B. Kohler, *Ann. Rev. Phys. Chem.*, 2009, **60**, 217–239.
- 25 S. K. Pal and A. H. Zewail, *Chem. Rev.*, 2004, **104**, 2099–2124.
- 26 B. Jayaram and T. Jain, *Annu. Rev. Biophys. Biomol. Struct.*, 2004, **33**, 343–361.

- 27 P. L. Privalov, A. I. Dragan, C. Crane-Robinson, K. J. Breslauer, D. P. Remeta and C. A. Minetti, *J. Mol. Biol.*, 2007, **365**, 1–9.
- 28 G. M. Spitzer, J. E. Fuchs, P. Markt, J. Kirchmair, B. Wellenzohn, T. Langer and K. R. Liedl, *Chem. Phys. Chem.*, 2008, **9**, 2766–2771.
- 29 E. Duboué-Dijon, A. C. Fogarty, J. T. Hynes and D. Laage, *J. Am. Chem. Soc.*, 2016, **138**, 7610–7620.
- 30 J. Poater, M. Swart, C. Fonseca Guerra and F. M. Bickelhaupt, *Chem. Comm.*, 2011, **47**, 7326–7328.
- 31 J. Poater, M. Swart, C. F. Guerra and F. M. Bickelhaupt, *Computational and Theoretical Chemistry*, 2012, **998**, 57–63.
- 32 J. Poater, M. Swart, F. M. Bickelhaupt and C. Fonseca Guerra, *Org. Biomol. Chem.*, 2014, **12**, 4691–4700.
- 33 T. A. Hamlin, J. Poater, C. Fonseca Guerra and F. M. Bickelhaupt, *Phys. Chem. Chem. Phys.*, 2017, **19**, 16969–16978.
- 34 P. Sharma, L. A. Lait and S. D. Wetmore, *Phys. Chem. Chem. Phys.*, 2013, **15**, 2435–2448.
- 35 P. Sharma, L. A. Lait and S. D. Wetmore, *Phys. Chem. Chem. Phys.*, 2013, **15**, 15538–15549.
- 36 D. J. Gibson and T. van Mourik, *Chem. Phys. Lett.*, 2017, **668**, 7–13.
- 37 B. J. R. Cuyacot, I. Durník, C. Foroutan-Nejad and R. Marek, *Journal of Chemical Information and Modelling*, 2021, **61**, 211–222.
- 38 M. Babinský, K. Bouzková, M. Pipška, L. Novosadová and R. Marek, *Journal of Physical Chemistry A*, 2013, **117**, 497–503.
- 39 K. V. Jovan Jose and K. Raghavachari, *Journal of Chemical Theory and Computation*, 2017, **13**, 1147–1158.
- 40 S. Miertus and J. Tomasi, *Chem. Phys.*, 1982, **65**, 239–245.
- 41 R. Cammi and J. Tomasi, *J. Comp. Chem.*, 1995, **16**, 1449–1458.
- 42 B. Mennucci, E. Cancès and J. Tomasi, *J. Phys. Chem. B*, 1997, **101**, 10506–10517.
- 43 M. Pecul and J. Sadlej, *Chem. Phys. Lett.*, 1999, **308**, 486–494.
- 44 V. Sychrovský, B. Schneider, P. Hobza, L. Židek and V. Sklenář, *Phys. Chem. Chem. Phys.*, 2003, **5**, 734–739.
- 45 P. Bouř, M. Buděšínský, V. Špirko, J. Kapitán, J. Šebestík and V. Sychrovský, *J. Am. Chem. Soc.*, 2005, **127**, 17079–17089.
- 46 M. L. McDermott, H. Vanselous, S. A. Corcelli and P. B. Petersen, *ACS central science*, 2017, **3**, 708–714.
- 47 N. Bhattacharjee and P. Biswas, *Biophysical Chemistry*, 2011, **158**, 73–80.
- 48 S. Tsuzuki, K. Honda, T. Uchimarui, M. Mikami and K. Tanabe, *J. Am. Chem. Soc.*, 2002, **124**, 104–112.
- 49 S. Grimme, J. Antony, T. Schwabe and C. Mück-Lichtenfeld, *Org. Biomol. Chem.*, 2007, **5**, 741–758.
- 50 S. Grimme, *Angew. Chem. Internat. Edit.*, 2008, **47**, 3430–3434.
- 51 R. Ditchfield, *J. Chem. Phys.*, 1972, **56**, 5688–5691.
- 52 K. Wolinski, J. F. Hinton and P. Pulay, *J. Am. Chem. Soc.*, 1990, **112**, 8251–8260.
- 53 T. Helgaker, P. J. Wilson, R. D. Amos and N. C. Handy, *J. Chem. Phys.*, 2000, **113**, 2983–2989.
- 54 S. Grimme, *J. Comput. Chem.*, 2006, **27**, 1787–1799.
- 55 T. Clark, J. Chandrasekhar, G. W. Spitznagel and P. R. J. Schleyer, *Comp. Chem.*, 1983, **4**, 294.
- 56 Aidas, K.; Angeli, C.; Bak, K. L.; Bakken, V.; Bast, R.; Boman, L.; Christiansen, O.; Cimiraglia, R.; Coriani, S.; Dahle, P.; Dalskov, E. K.; Ekström, U.; Enevoldsen, T.; Eriksen, J. J.; Ettenhuber, P.; Fernández, B.; Ferrighi, L.; Fliegl, H.; Frediani, L.; Hald, K.; Halkier, A.; Hättig, C.; Heiberg, H.; Helgaker, T.; Hennum, A. C.; Hettema, H.; Hjertenæs, E.; Høst, S.; Høyvik, I.-M.; Iozzi, M. F.; Jansik, B.; Jensen, H. J. Aa.; Jonsson, D.; Jørgensen, P.; Kauczor, J.; Kirpekar, S.; Kjærgaard, T.; Klopper, W.; Knecht, S.; Kobayashi, R.; Koch, H.; Kongsted, J.; Krapp, A.; Kristensen, K.; Ligabue, A.; Lutnæs, O. B.; Melo, J. I.; Mikkelsen, K. V.; Myhre, R. H.; Neiss, C.; , Nielsen, C. B.; Norman, P.; Olsen, J.; Olsen, J. M. H.; Osted, A.; Packer, M. J.; Pawłowski, F.; Pedersen, T. B.; Provasi, P. F.; Reine, S.; Rinkevicius, Z.; Ruden, T. A.; Ruud, K.; Rybkin, V.; Salek, P.; Samson, C. C. M.; Sánchez de Merás, A.; Saue, T.; Sauer, S. P. A.; Schimmelpfennig, B.; Sneskov, K.; Steinda, A. H.; Sylvester-Hvid, K. O.; Taylor, P. R.; Teale, A. M.; Tellgren, E. I.; Tew, D. P.; Thorvaldsen, A. J.; Thøgersen, L.; Vahtras, O.; Watson, M. A.; Wilson, D. J. D.; Ziolkowski, M.; Ågren, H. , The Dalton quantum chemistry program system, *WIREs Comput. Mol. Sci.* 2014, 4:269–284 (doi: 10.1002/wcms.1172).
- 57 M. J. Abraham, T. Murtola, R. Schulz, S. Páll, J. C. Smith, B. Hess and E. Lindahl, *SoftwareX*, 2015, **1-2**, 19–25.
- 58 W. D. Cornell, P. Cieplak, C. I. Bayly, I. R. Gould, K. M. Merz, D. M. Ferguson, D. C. Spellmeyer, T. Fox, J. W. Caldwell and P. A. Kollman, *J. Am. Chem. Soc.*, 1995, **117**, 5179–5197.
- 59 B. Hess, H. Bekker, H. J. C. Berendsen and J. G. E. M. Fraaije, *Journal of Computational Chemistry*, 1997, **18**, 1463–1472.
- 60 H. J. C. Berendsen, J. P. M. Postma, W. F. van Gunsteren, A. DiNola and J. R. Haak, *The Journal of Chemical Physics*, 1984, **81**, 3684–3690.
- 61 S. Standara, K. Bouzková, M. Straka, Z. Zacharová, K. Hocek, J. Marek and R. Marek, *Physical Chemistry Chemical Physics*, 2011, **13**, 15854–15864.
- 62 A. Frank, I. Onila, H. M. Möller and T. E. Exner, *Proteins*, 2011, **79**, 2189–2202.
- 63 A. Frank, H. M. Möller and T. E. Exner, *J. Chem. Theory and Comput.*, 2012, **8**, 1480–1492.
- 64 T. E. Exner, A. Frank, I. Onila and H. M. Möller, *J. Chem. Theory and Comput.*, 2012, **8**, 4818–4827.
- 65 P. N. Borer, S. R. LaPlante, N. Zanatta and G. C. Levy, *Nucleic acids research*, 1988, **16**, 2323–2332.
- 66 K. Malináková, L. Novosadová, M. Lahtinen, E. Kolehmainen, J. Brus and R. Marek, *The Journal of Physical Chemistry A*, 2010, **114**, 1985–1995.
- 67 G. Colherinhas, L. B. A. Oliveira, M. A. Castro, T. L. Fonseca, K. Coutinho and S. Canuto, *Journal of Molecular Liquids*, 2019, **294**, 111611.
- 68 M. Yoosefian and A. Mola, *Journal of Molecular Liquids*, 2015, **209**, 526–530.